Experimental Comparison of Passive and Synchronous Rectification on a Locally Manufactured Small Wind Turbine

Adrien Prévost, Romain Delpoux, Vincent Léchappé, Kostas Latoufis, Xavier Brun

Experimental Comparison of Passive and Synchronous Rectification on a Locally Manufactured Small Wind Turbine

Adrien Prévost
Univ Lyon, INSA Lyon
Universite Claude Bernard Lyon 1,
Ecole Centrale de Lyon,
Laboratoire Ampere CNRS UMR 5005
Villeurbanne, France
adrien.prevost@insa-lyon.fr

Romain Delpoux
Univ Lyon, INSA Lyon
Universite Claude Bernard Lyon 1,
Ecole Centrale de Lyon,
Laboratoire Ampere CNRS UMR 5005
Villeurbanne, France
romain.delpoux@insa-lyon.fr

Vincent Léchappé
Univ Lyon, INSA Lyon
Universite Claude Bernard Lyon 1,
Ecole Centrale de Lyon,
Laboratoire Ampere CNRS UMR 5005
Villeurbanne, France
vincent.lechappe@insa-lyon.fr

Kostas Latoufis
Department of Electrical
and Computer Engineering
National Technical University of Athens
Athens, Greece
latoufis@power.ece.ntua.gr

Xavier Brun
Univ Lyon, INSA Lyon
Universite Claude Bernard Lyon 1,
Ecole Centrale de Lyon,
Laboratoire Ampere CNRS UMR 5005
Villeurbanne, France
xavier.brun@insa-lyon.fr

***Abstract*—In this article, synchronous rectification was studied as a solution to increase the energy yield of battery connected Locally Manufactured Small Wind Turbines (LMSWTs). An analytical expression to determine the necessary battery voltage for synchronous rectification on the LMSWT Permanent Magnets Synchronous Generator (PMSG) was derived. It was found that the battery voltage for synchronous rectification should be two times higher than that of the passive strategy for an identical generator. The performance of the LMSWT under synchronous rectification with Field Oriented Control (FOC) and Optimal Torque (OT) Maximum Power Point Tracking (MPPT) was measured experimentally on a real scale wind turbine emulator under steady wind conditions. It was found that for the passive Diode Rectifier (DR) configuration, the Annual Energy Production (AEP) estimation was $(16-38\%)$ lower than for the synchronous rectification strategy.**

***Index Terms*—Locally manufactured small wind turbines, Maximum power point tracking, Synchronous rectification**

I. Introduction

Small scale ($<$ 20 kW) Wind Energy Conversion Systems (WECSs) are mainly used for rural electrification in remote areas or residential behind-the-meter grid connected application. Locally Manufactured Small Wind Turbines (LMSWTs) are identified as an adequate technology for sustainable rural electrification. Following robust designs [1] ranging from 1.2 to 4.2 m rotor diameter, these horizontal axis wind turbines are made of fixed pitch wooden blades mounted on an axial flux PMSG. A passive furling system acts as a mechanical protection by introducing a yaw angle for strong winds. By definition, LMSWTs could be entirely manufactured by rural communities with basic tools which facilitates the technology adoption and its maintenance [2]. Additionally, they benefit from a lower Levelized Cost Of Energy (LCOE) than similar scale commercial wind turbines in low mean wind speed ($<$ 6 m/s) areas [3]. This is mainly due to their low capital and maintenance costs as well as their good performance at low wind speeds. A way to further reduce the LCOE of LMSWTs is to increase their energy yield by optimizing elements of the power conversion chain. A typical power conversion chain of a battery-connected LMSWT is represented in Fig. 1(a). In the original configuration, the PMSG is connected to a battery through a passive DR. This configuration does not allow MPPT since the DC voltage of the battery is almost constant which imposes a unique torque-speed trajectory to the generator [4].

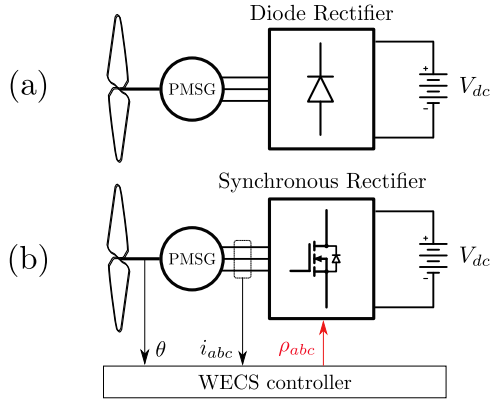

Fig. 1. Locally manufactured small wind turbine system architecture with a diode rectifier (a) or a synchronous rectifier (b).

However, it is possible to optimize the matching between subsystem elements such as blades, generator, transmission lines and battery voltage through a holistic design [5]. This approach can lead to a behavior close to MPPT over a certain range of wind speeds. However, the DR introduces significant power losses in the system, mainly through the induced current harmonics in the generator and the diodes' conduction. The replacement of the DR by an active Synchronous Rectifier (SR) in standalone Small Wind Turbines (SWTs) systems has been studied in the literature [6]–[8]. It enables a precise control of the generator torque through FOC and the implementation of a MPPT algorithm. The associated architecture is represented in Fig. 1(b) where the measurements of line currents and angular position are required by the WECS controller. To our knowledge, the impact of such a conversion strategy has not been studied for LMSWTs.

The goal of this article is to evaluate experimentally the performance of a vector controlled SR on a battery-connected LMSWT system. Its performance will be compared with the original passive DR strategy in terms of aerodynamic operating points, efficiencies, power curves and AEP. In this scope, a wind turbine emulator has been constructed [9] and connected with a real scale LMSWT generator.

In Section II, the LMSWT system is modelled for both active and passive rectifier configurations. The condition on the necessary battery voltage to enable the comparison of both strategies on the same generator is derived. Section III presents the experimental setup composed of a wind turbine emulator test bed. In addition, the measurement protocol is also presented. Finally, the experimental results are presented in Section IV for both strategies and then discussed.

II. System overview

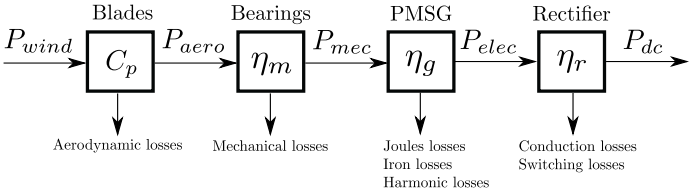

Fig. 2. Overview of the system power conversion chain elements with their losses and efficiencies.

The power conversion chain of the LMSWT system is represented in Fig. 2 by an efficiency for each conversion element and the corresponding losses.

A. Aerodynamics

The aerodynamic efficiency of the wind turbine rotor is commonly modelled with the aerodynamic coefficient C_p which enables to write a static expression of the power extracted from the wind by the blades

$$P_{aero} = \frac{1}{2}\rho_{air} A V_w^3 C_p(\lambda) = P_{wind} \cdot C_p(\lambda), \tag{1}$$

with A the rotor swept area, ρ_{air} the air density and V_w the wind velocity.

LMSWTs blades have a fixed pitch, thus C_p varies in one dimension according to the Tip Speed Ratio (TSR) λ written as

$$\lambda = \frac{\omega \cdot R}{V_w} \tag{2}$$

where ω is the rotor angular velocity and R the rotor radius.

The aerodynamic coefficient of the LMSWT is represented in Fig. 3. It has been computed from real test site experimental data at the National Technical University of Athens, Greece.

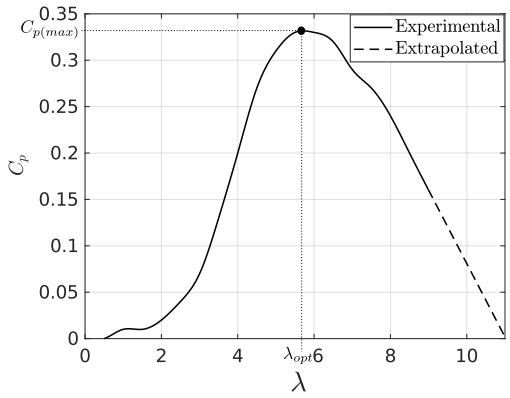

Fig. 3. LMSWT aerodynamic coefficient in function of TSR.

By conservation of power, the aerodynamic torque applied by the blades on the shaft can be written as

$$\tau_b = \frac{P_{aero}}{\omega}. \tag{3}$$

B. Generator

The generator topology used in the LMSWT is an axial flux surface mounted PMSG with air-cored non-overlapping concentrated windings. The corresponding voltage equations in the reference rotating frame $d-q$ are given by [10, p.232]

$$\begin{aligned} v_d &= R_s i_d + L_s \tfrac{di_d}{dt} - p\omega L_s i_q, \\ v_q &= R_s i_q + L_s \tfrac{di_q}{dt} + p\omega L_s i_d + p\phi_f \omega \end{aligned} \tag{4}$$

with R_s the phase resistance, L_s the phase inductance, ϕ_f the peak magnetic flux of the permanent magnets seen by a stator phase winding, p the pole pairs number and ω the rotational velocity. Since Clarke's transform is used, amplitudes are conserved which enables to write the phase voltage amplitude as

$$V = \sqrt{v_d^2 + v_q^2}. \tag{5}$$

The electromagnetic torque of the PMSG is proportional to the quadrature axis current according to

$$\tau_g = \frac{3}{2} p \phi_f i_q. \tag{6}$$

C. Rectifier and battery interaction

Let us define m as the ratio between the battery voltage and the line voltage amplitude, expressed as

$$m = \frac{V_{dc}}{V}. \tag{7}$$

This ratio will be explicated in the case of the SR (m_{SR}) and DR (m_{DR}).

1) Diode Rectifier: The diodes within the passive rectifier starts conducting when the line to line voltage amplitude exceeds the DC-link voltage value, which means when the condition

$$\sqrt{3}V > V_{dc} \tag{8}$$

is met. Hence the voltage ratio in the case of the DR is constrained by

$$m_{DR} < \sqrt{3}. \tag{9}$$

The evolution of the power transfer through the DR in function of m_{DR} and the internal impedance of the generator can be determined [4] but will not be analyzed in detail here. We emphasize the fact that there is no power transfer possible unless $m_{DR} < \sqrt{3}$.

2) Synchronous Rectifier: The active rectifier used in this work is a classical three legs with two levels voltage source converter. The theoretical maximum sinusoidal phase voltage amplitude V_{max} achievable by this converter structure is given by

$$V_{max} = \frac{V_{dc}}{\sqrt{3}} \geq V. \tag{10}$$

This could be achieved with space vector Pulse Width Modulation (PWM) [11] which is used in this work. This leads to a voltage ratio constrained by

$$m_{SR} > \sqrt{3}. \tag{11}$$

At this stage, it is essential to note that the necessary conditions needed on the battery voltage level for the functioning of the diode and synchronous rectifiers are not compatible. Indeed, from the analysis of (9) and (11) it can be concluded that

$$m_{DR} < m_{SR}. \tag{12}$$

This highlights the fact that for a given mechanical operating point of an identical PM machine, the two rectifiers require a different DC-link voltage level to apply the same torque at a given rotational velocity. Thus, reaching an identical WECS aerodynamic operating point (τ_b, ω) implies a specific DC-link voltage value for the passive rectifier, which is systematically lower than the minimal value required to perform synchronous PWM rectification. Hence, to be able to test the SR on the LMSWT generator, the battery voltage should be adapted. The DC voltage at the SR must be calculated by taking into account the WECS control strategy.

D. WECS control strategy

The WECS control strategy chosen in this work is called Optimal Torque (OT) control which has imposed itself as a standard in variable speed wind turbines. This simple control method benefits from strong stability proofs and is tolerant to aerodynamic model uncertainties [12]. In spite of its sensitivity to high inertia, it can lead to the optimal power in steady state while ensuring smooth shaft loads during transients. Moreover, it can be coupled to an optimization scheme to compensate model uncertainties, which makes OT a good candidate for LMSWTs. In this article, the aerodynamic model is known and steady state operating points are considered. Hence, the original OT scheme is used, which consists in tracking the generator reference torque $\tau_g^{\#}$ according to the law

$$\tau_g^{\#} = -K\omega^2 \tag{13}$$

with K the torque gain. The use of a SR enables FOC which allows controlling the generator torque through the quadrature axis current using eq. (6). This well-established method [13] will not be developed in this article. The gain K leading to the optimal aerodynamic torque is denoted K_{aero} and can be derived by inserting (1) and (2) in (3)

$$K_{aero} = \frac{1}{2}\rho_{air} A R^3 \frac{C_{p(max)}}{\lambda_{opt}^3} \tag{14}$$

with $C_{p(max)}$ the maximum power coefficient that occurs at the optimal TSR λ_{opt}. In steady wind conditions, following the control law (13) leads the wind turbine to the optimal TSR [12]. Hence, at the rated wind speed $V_{w(rated)}$, the corresponding rated rotational velocity ω_r could be calculated from (2)

$$\omega_r = \frac{\lambda_{opt} \cdot V_{w(rated)}}{R}. \tag{15}$$

Operating conditions above the rated wind speed should take into account the furling behavior of the wind turbine, which is out of the scope of this article.

E. Battery voltage

It is known that the voltage of a typical 24V lead-acid battery bank can vary from around 22V to 28V according to its state of charge and temperature. In this work, the evolution of battery voltage will be modelled by a DC load with a constant DC voltage.

1) DR battery voltage: The generator used for the LMSWT under study has been designed for a DR connected to a 24 V battery pack. This system configuration will be tested under several fixed battery voltages between 22 and 28V to evidence the voltage influence on the global impedance matching.

2) SR battery voltage: An analytical expression of the static constraint on V_{dc} could be established by inserting eqs. (6) and (4) in eq. (5), leading to

$$V_{max} \geq \sqrt{\left(\frac{2\tau_g}{3p\phi_f}\right)^2 \cdot (R_s^2 + (p\omega L_s)^2) + (p\phi_f\omega)^2 + \frac{4R_s\tau_g\omega}{3}} \tag{16}$$

where the flux weakening possibility is excluded from the analysis, meaning that $i_d = 0$. To determine the constraint on the battery voltage under active rectification at rated wind speed, one should solve (16) with the values of $\omega = \omega_r$ and $\tau_g = -K\omega_r^2$. Hence, by inserting (16) in (10), the minimum battery DC voltage required for performing synchronous rectification at rated wind speed can be calculated with

$$V_{dc} \geq \sqrt{3}\omega_r \sqrt{(p\phi_f)^2 - \frac{4}{3}R_s\omega_r K - \frac{2K}{3p\phi_f}\left(R_s^2 + (pL_s\omega_r)^2\right)}. \tag{17}$$

This equation can be used to check if a battery voltage is high enough to enable a synchronous rectified generator to match a set of blades. In the scope of this article, we have used it to determine the required DC voltage for the experimental comparison. The computation of eq. (17) with the LMSWT system parameters gives a DC voltage of 48V, which is two times the battery voltage of the passive system original design.

III. Experimental setup

As a recall, the goal of the experimental setup is to be able to measure a static power curve of a LMSWT with a real scale generator, under passive and active rectification. The choice of employing a Wind Turbine Emulator (WTE) test bed has been made to be able to conduct the tests in a laboratory.

A. The test bench architecture

A picture of the emulator test bed is shown in Fig. 4. It is made of a Permanent Magnets Synchronous Motor (PMSM) which is controlled to emulate the torque applied by the blades on the generator. The PMSM is mechanically connected to a 700W rated power LMSWT generator through a Torque Meter (TM) which measures the shaft torque, angular velocity and position. The PMSG is connected to the DR or SR alternatively. The rectifier is directly connected to the DC load which regulates the DC-link voltage. The generator phase currents as well as DC-link voltage and rectifier output DC current are measured. The software layers are embedded in a dSPACE controller which ensures the measurements acquisition and synthesis of control signals. The test bed full architecture and control schemes are detailed in [9].

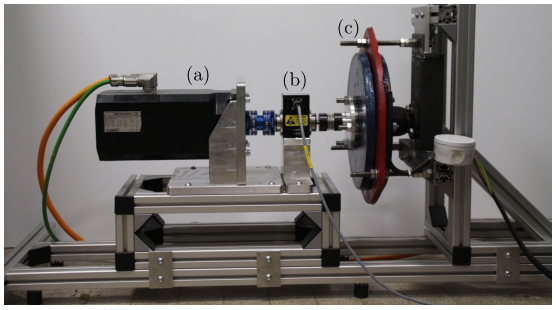

Fig. 4. The WECS emulator test bed : (a) PMSM, (b) TM, (c) PMSG.

B. Experimental framework

Using eqs. (1), (2), (3) and the LMSWT $C_p(\lambda)$ characteristic of Fig. 3, the motor torque τ_m is controlled in real time to apply the aerodynamic torque of the blades on the PMSG. Wind velocities from cut-in (3 m/s) to rated (10 m/s) by steps of 0.5 m/s are successively applied to the emulator test bed. For both rectifier configurations, the torque and rotational velocity are measured by the TM, as well as the DC current and voltage. All measurements are averaged over a 5s period. From these measurements, it is possible to deduce the Generator-Rectifier efficiency defined by

$$\eta = \eta_m \cdot \eta_g \cdot \eta_r = \frac{P_{dc}}{P_{aero}} = \frac{V_{dc} \cdot I_{dc}}{\tau_b \cdot \omega}. \tag{18}$$

This metric will be used to analyze the results.

IV. Experimental results

A. Optimal torque gain under synchronous rectification

The OT control law optimizes the aerodynamic power P_{aero} only and does not take into account the mechanical, generator and rectifier losses, as it can be seen on the power conversion chain in Fig. 2. Hence, the maximum aerodynamic power does not necessarily lead to the maximum electrical power output [14]. That is why a first experiment to characterize the DC power in function of the torque gain K has been conducted under active rectification for low, medium and high wind speeds (5, 7 and 9 m/s). The results are represented in Fig. 5 where each DC power curve is normalized by its maximum. It can be observed that for the three wind speeds, the maximum power is reached with a torque gain that is less important than the K_{aero} computed analytically with eq. (14). The gain K_{dc} which maximizes the DC power was found experimentally to be a good compromise for all three wind speeds. It is located on the left of K_{aero} in Fig. 5.

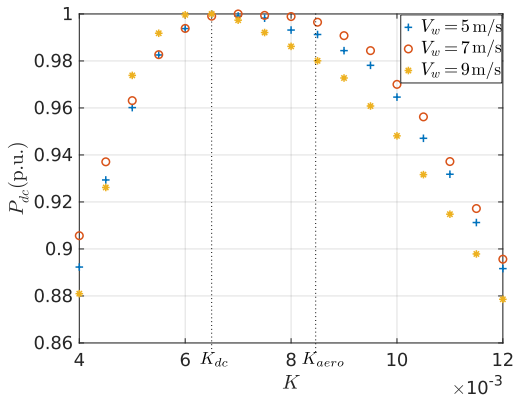

Fig. 5. Cartography of the DC power output in function of the gain K.

B. Aerodynamic behavior

1) Diode rectifier: PMSG based small wind turbines directly connected to a battery through a DR almost operate at a constant rotational velocity. Hence, as the wind speed

increases, the TSR decreases. This is well illustrated by Fig. 6. It can be observed that the cut-in (i.e. at $V_w = 3$ m/s) TSR is affected by the battery voltage. A higher battery voltage leads to a higher cut-in TSR. Indeed, to start transferring power, the DR needs to respect the condition of eq. (9) which is verified at higher rotational velocities as the DC voltage increases. For each battery voltage, there is a wind speed for which the TSR is optimal and hence C_p maximized. It can be seen from Fig. 7 that a low battery level (22V-24V) maximizes C_p around low wind speeds (i.e. 5 m/s). The wind speed at which C_p is maximized shifts to the right as the battery voltage increases.

2) Synchronous rectifier: From Fig. 7, one can remark that K_{dc} and K_{aero} both leads to a similar C_p, very close to the optimal value for all wind speeds. From Fig. 6 it can be seen that the gain K_{dc} leads to a TSR around 6 which is higher than the value of 5.7 obtained with K_{aero}. Indeed, for a given wind speed, a lower torque gain K results in a lower torque demand from the controller, leading the rotor to a higher rotational speed operating point.

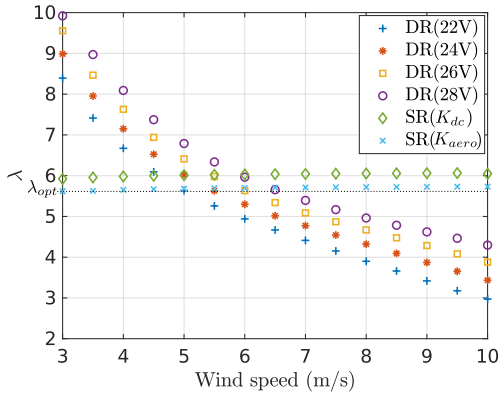

Fig. 6. Wind turbine TSR operating points.

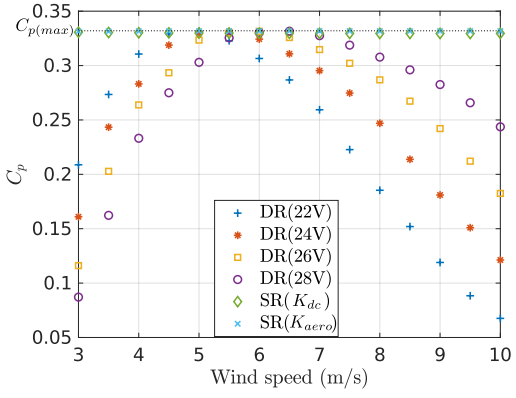

Fig. 7. Wind turbine aerodynamic coefficient operating points under diode rectification and synchronous rectification.

C. Generator-Rectifier efficiency

The Generator-Rectifier efficiency η takes into account all the losses between P_{aero} and P_{dc}. Hence, it depends on the mechanical and electrical operating points. It can be observed in Fig. 8 that the combination of MPPT control and synchronous rectification systematically leads to a better efficiency. Considering the SR, the torque gain K_{dc} leads to a slightly better efficiency, which is more remarkable for high wind speeds. The measurement and modelling of the individual losses could provide further information about the reasons of this gain in terms of efficiency.

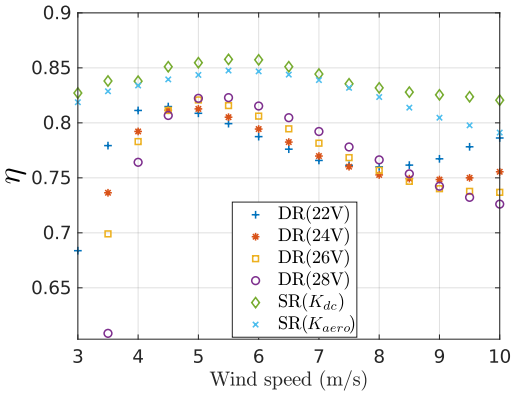

Fig. 8. Generator-Rectifier subsystem efficiency operating points under diode rectification and synchronous rectification.

D. Power curves and annual energy production

The power curves are plotted in Fig. 9 for each system configuration. An estimation of the Annual Energy Production (AEP) has been calculated from the obtained power curves, considering a Rayleigh distribution with a mean wind speed of 5 m/s, which is typical for a small wind turbine site. Only the wind speeds between 3 and 10 m/s have been taken into account in the AEP calculation, since the furling behavior is difficult to predict. However, with such a distribution, there is a 96% probability that $V_w < 10$ m/s which makes the calculation realistic. The results of the AEP estimation is represented in Fig. 10 as a bar graph. The ratio to the SR(K_{dc}) AEP is given on the top of each bar to help the comparison. The SR(K_{aero}) power curve is from 0 to 2% below the SR(K_{dc}) which leads to an 1% lower AEP prediction. As for the DR configuration, the power curves are very dependent on the battery voltage. In the low wind speed zone (between 4 and 6 m/s), they are fairly similar to the SR power curve. For high wind speeds, they differ more from each other. For a high battery voltage the estimated AEP is 16% lower than for the SR(K_{dc}) energy yield while it is even lower (38%) for a low battery voltage. Interestingly, with a passive DR configuration, a battery that tends to be in a discharged state will tend to harvest less energy than a charged battery, at least in the initial stages of charging.

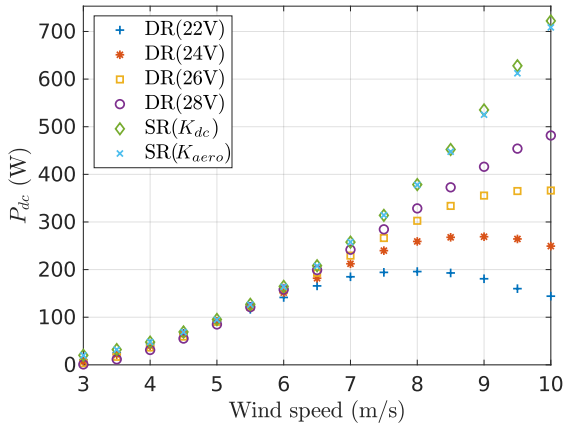

Fig. 9. Wind turbine power curves of the system under diode rectification and synchronous rectification.

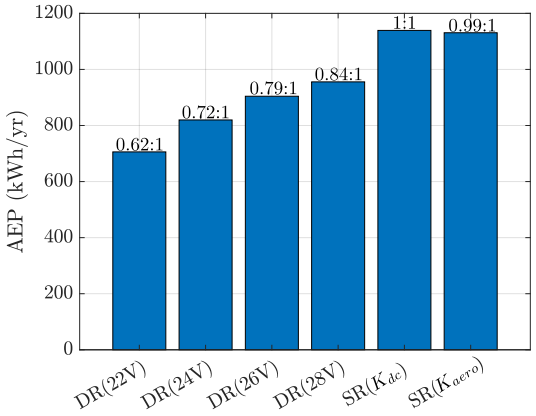

Fig. 10. Prediction of the AEP with a Rayleigh distribution at 5 m/s average wind speed.

V. Conclusion

In this article, synchronous rectification was studied as a solution to increase the energy yield for battery connected LMSWTs. First, an analytical expression to determine the necessary battery voltage for synchronous rectification on the LMSWT generator was derived. It was found that the battery voltage for synchronous rectification should be two times higher than for the passive strategy. Then, the performance of the LMSWT under synchronous rectification was evaluated experimentally on a real scale wind turbine emulator under steady wind conditions. To do so, an optimal torque control MPPT strategy was implemented and tested with two different torque gains. One (K_{dc}) maximizes the overall DC power output while the other (K_{aero}) the aerodynamic power. It results that the difference in the estimated AEP between the two different gains is about 1%. These results were compared with the performance of the passive DR configuration. It was evidenced that for the latter configuration, the AEP estimation is $(16-38\%)$ lower than for the SR configuration, depending on the battery voltage.

Taking a step back from these figures, it should be reminded that even if the wind turbine emulator is real scale setup, the real performance of the DR could be measured on a wind turbine test site only. A more accurate energy prediction could be obtained from dynamic tests on the emulator. Moreover, to lead a fairer comparison, a generator could be specifically optimized for active rectification to enable the experiments on identical battery voltages. Finally, to evaluate if this synchronous rectification strategy is worth the extra complexity and cost in terms of LCOE, a study over the LMSWT life cycle should be conducted. These are future perspectives to this work.

Acknowledgment

The authors would like to thank Jay Hudnall for providing the LMSWT generator.

References

[1] H. Piggott, *A Wind Turbine Recipe Book*, 2009.
[2] K. C. Latoufis, T. V. Pazios, and N. D. Hatziargyriou, "Locally Manufactured Small Wind Turbines: Empowering communities for sustainable rural electrification." *IEEE Electrification Magazine*, vol. 3, no. 1, pp. 68–78, Mar. 2015.
[3] J. Sumanik-Leary, H. Piggott, R. Howell, and A. While, "Locally manufactured small wind turbines, how do they compare to commercial machines ?" *Proceedings of 9th PhD Seminar on Wind Energy in Europe*, p. 5, 2013.
[4] M. F. Iacchetti, G. M. Foglia, A. Di Gerlando, and A. J. Forsyth, "Analytical Evaluation of Surface-Mounted PMSG Performances Connected to a Diode Rectifier," *IEEE Transactions on Energy Conversion*, vol. 30, no. 4, pp. 1367–1375, Dec. 2015.
[5] K. Latoufis, G. Serafeim, K. Chira, V. Riziotis, S. Voutsinas, and N. Hatziargyriou, "Holistic Design of Small-scale Stand-alone Wind Energy Conversion Systems Using Locally Manufactured Small Wind Turbines," *Journal of Physics: Conference Series*, vol. 1618, p. 042012, Sep. 2020.
[6] A. Mirecki, X. Roboam, and F. Richardeau, "Architecture Complexity and Energy Efficiency of Small Wind Turbines," *IEEE Transactions on Industrial Electronics*, vol. 54, no. 1, pp. 660–670, Feb. 2007.
[7] R. Aubrée, F. Auger, M. Macé, and L. Loron, "Design of an efficient small wind-energy conversion system with an adaptive sensorless MPPT strategy," *Renewable Energy*, vol. 86, pp. 280–291, Feb. 2016.
[8] C. J. J. Labuschagne and M. J. Kamper, "Design Optimisation and Comparison of Non-overlap Winding PM Wind Generators for Active and Passive Battery Charging Systems," in *2018 XIII International Conference on Electrical Machines (ICEM)*. Alexandroupoli: IEEE, Sep. 2018, pp. 690–696.
[9] A. Prévost, V. Léchappé, R. Delpoux, and X. Brun, "An emulator for static and dynamic performance evaluation of small wind turbines," in *2023 IEEE 32nd International Symposium on Industrial Electronics (ISIE)*. Helsinki-Espoo: IEEE, Jun. 2023.
[10] J. F. Gieras, R.-J. Wang, and M. J. Kamper, *Axial Flux Permanent Magnet Brushless Machines*, 2nd ed. Springer Netherlands, 2008.
[11] J. Holtz, W. Lotzkat, and A. M. Khambadkone, "On Continuous Control of PWM Inverters in the Overmodulation Range Including the Six-Step Mode," *IEEE Transactions on Power Electronics*, vol. 8, no. 4, 1993.
[12] K. E. Johnson, "Control of variable-speed wind turbines: standard and adaptive techniques for maximizing energy capture," *IEEE Control Systems*, vol. 26, no. 3, pp. 70–81, 2006.
[13] J.-N. Chiasson, *Modeling and High-Performance Control of Electric Machines*, ieee press ed., 2005.
[14] J. D. De Kooning, T. L. Vandoorn, J. Van de Vyver, B. Meersman, and L. Vandevelde, "Displacement of the maximum power point caused by losses in wind turbine systems," *Renewable Energy*, vol. 85, pp. 273–280, Jan. 2016.